

Distribution patterns of intramyocellular and extramyocellular fat by magnetic resonance imaging in subjects with diabetes, prediabetes and normoglycaemic controls

Lena S. Kiefer, Jana Fabian, Susanne Rospleszcz, Roberto Lorbeer, Jürgen Machann, Mareen S. Kraus, Frank Roemer, Wolfgang Rathmann, Christa Meisinger, Margit Heier, Konstantin Nikolaou, Annette Peters, Corinna Storz, Thierno D. Diallo, Christopher L. Schlett, Fabian Bamberg


Angaben zur Veröffentlichung / Publication details:

Kiefer, Lena S., Jana Fabian, Susanne Rospleszcz, Roberto Lorbeer, Jürgen Machann, Mareen S. Kraus, Frank Roemer, et al. 2021. "Distribution patterns of intramyocellular and extramyocellular fat by magnetic resonance imaging in subjects with diabetes, prediabetes and normoglycaemic controls." *Diabetes, Obesity and Metabolism* 23 (8): 1868–78. <https://doi.org/10.1111/dom.14413>.

ORIGINAL ARTICLE

WILEY

Distribution patterns of intramyocellular and extramyocellular fat by magnetic resonance imaging in subjects with diabetes, prediabetes and normoglycaemic controls

Lena S. Kiefer MD¹  | Jana Fabian BS¹ | Susanne Rospleszcz PhD^{2,3} | Roberto Lorbeer PhD^{4,5} | Jürgen Machann PhD^{6,7,8} | Mareen S. Kraus MD¹ | Frank Roemer MD^{9,10} | Wolfgang Rathmann MD, MSPH^{8,11} | Christa Meisinger MPH^{12,13} | Margit Heier PhD^{3,14} | Konstantin Nikolaou MD¹ | Annette Peters PhD^{2,3,5,8} | Corinna Storz MD¹⁵ | Thierno D. Diallo MD¹⁶ | Christopher L. Schlett MD¹⁶ | Fabian Bamberg MD¹⁶

¹Department of Diagnostic and Interventional Radiology, University of Tuebingen, Tuebingen, Germany

²Epidemiology, Ludwig-Maximilians-University München, Munich, Germany

³German Research Center for Environmental Health, Institute of Epidemiology, Helmholtz Zentrum München, Neuherberg, Germany

⁴Department of Radiology, Ludwig-Maximilians-University Hospital, Munich, Germany

⁵German Centre for Cardiovascular Research (DZHK e.V.), Munich, Germany

⁶Section on Experimental Radiology, Department of Diagnostic and Interventional Radiology, University of Tuebingen, Tuebingen, Germany

⁷Institute for Diabetes Research and Metabolic Diseases (IDM) of the Helmholtz Center Munich at the University of Tuebingen, Tuebingen, Germany

⁸German Center for Diabetes Research (DZD), Tuebingen, Germany

⁹Department of Radiology, University of Erlangen-Nuremberg, Erlangen, Germany

¹⁰Department of Radiology, Boston University School of Medicine, Boston, Massachusetts

¹¹German Diabetes Center, Institute for Biometrics and Epidemiology, Duesseldorf, Germany

¹²Epidemiology, University Hospital Augsburg, Augsburg, Germany

¹³German Research Center for Environmental Health, Independent Research Group Clinical Epidemiology, Helmholtz Zentrum München, Neuherberg, Germany

¹⁴KORA Study Centre, University Hospital Augsburg, Augsburg, Germany

¹⁵Department of Neuroradiology, Medical Center, Faculty of Medicine, University of Freiburg, Freiburg, Germany

¹⁶Department of Diagnostic and Interventional Radiology, University Medical Center Freiburg, Faculty of Medicine, University of Freiburg, Freiburg, Germany

Correspondence

Lena S. Kiefer, MD, Department of Diagnostic and Interventional Radiology, University of Tuebingen, Hoppe-Seyler-Strasse 3, 72076 Tuebingen, Germany.
Email: lena.kiefer@med.uni-tuebingen.de

Abstract

Aim: To evaluate the distribution of intramyocellular lipids (IMCLs) and extramyocellular lipids (EMCLs) as well as total fat content in abdominal skeletal muscle by magnetic resonance imaging (MRI) using a dedicated segmentation algorithm in subjects with type 2 diabetes (T2D), prediabetes and normoglycaemic controls.

Materials and Methods: Subjects from a population-based cohort were classified with T2D, prediabetes or as normoglycaemic controls. Total myosteatosis, IMCLs and

This is an open access article under the terms of the Creative Commons Attribution-NonCommercial-NoDerivs License, which permits use and distribution in any medium, provided the original work is properly cited, the use is non-commercial and no modifications or adaptations are made.

© 2021 The Authors. *Diabetes, Obesity and Metabolism* published by John Wiley & Sons Ltd.

EMCLs were quantified by multiecho Dixon MRI as proton-density fat-fraction (in %) in abdominal skeletal muscle.

Results: Among 337 included subjects (median age 56.0 [IQR: 49.0-64.0] years, 56.4% males, median body mass index [BMI]: 27.2 kg/m²), 129 (38.3%) were classified with an impaired glucose metabolism (T2D: 49 [14.5%]; prediabetes: 80 [23.7%]). IMCLs were significantly higher than EMCLs in subjects without obesity (5.7% [IQR: 4.8%-7.0%] vs. 4.1% [IQR: 2.7%-5.8%], $P < .001$), whereas the amounts of IMCLs and EMCLs were shown to be equal and significantly higher in subjects with obesity (both 6.7%, $P < .001$). Subjects with prediabetes and T2D had significantly higher amounts of IMCLs and EMCLs compared with normoglycaemic controls ($P < .001$). In univariable analysis, prediabetes and T2D were significantly associated with both IMCLs (prediabetes: β : 0.76, 95% CI: 0.28-1.24, $P = .002$; T2D: β : 1.56, 95% CI: 0.66-2.47, $P < .001$) and EMCLs (prediabetes: β : 1.54, 95% CI: 0.56-2.51, $P = .002$; T2D: β : 2.15, 95% CI: 1.33-2.96, $P < .001$). After adjustment for age and gender, the association of IMCLs with prediabetes attenuated ($P = 0.06$), whereas for T2D, both IMCLs and EMCLs remained significantly and positively associated ($P < .02$).

Conclusion: There are significant differences in the amount and distribution ratio of IMCLs and EMCLs between subjects with T2D, prediabetes and normoglycaemic controls. Therefore, these patterns of intramuscular fat distribution by MRI might serve as imaging biomarkers in both normal and impaired glucose metabolism.

KEYWORDS

body composition, cohort study, type 2 diabetes

1 | INTRODUCTION

Insulin resistance is considered the major feature in the pathophysiology of type 2 diabetes (T2D).¹ In general, lipids such as triglycerides interfere with peripheral insulin signalling by competing with glucose for energy production.² Thereby, increased levels of circulating plasma lipids inhibit insulin-stimulated, peripheral glucose metabolism, consistent with an increased peripheral insulin resistance.^{3,4} However, not only higher levels of circulating plasma lipids but also increased ectopic lipid deposits within peripheral organs are considered causal factors in the development of insulin resistance.^{3,5} Because skeletal muscle is the primary organ accounting for the whole-body insulin-stimulated glucose disposal, peripheral insulin sensitivity mainly depends on glucose utilization in skeletal muscle tissue. Thus, even minor changes in skeletal muscle composition regarding fat content and lipid distribution may be key factors contributing to the pathogenesis of insulin resistance and T2D.^{6,7}

Intramuscular fat may be deposited in two distinct compartments, either as intramyocellular lipids (IMCLs) accumulated in the cytoplasm of myocytes or as extramyocellular lipids (EMCLs) in interstitial, intramyofascial adipocytes. They differ essentially regarding their chemical reactivity, with EMCLs being metabolically rather inert and IMCLs, by contrast, being characterized by a rapid cycle of storage, mobilization and usage as a fast available source of energy.^{8,9} Recent data suggest a correlation of insulin resistance and IMCLs rather than

EMCLs in subjects with normoglycaemia and diabetes as well as in subjects with and without obesity.¹⁰ Furthermore, the amount of IMCLs has been described as a promising predictor and potential marker for muscular insulin resistance.^{7,11,12}

In the past, reliable quantification of skeletal muscle fat content was only possible *ex vivo* by invasive techniques (histopathology). However, non-invasive methodologies using magnetic resonance (MR), such as single-voxel proton-MR spectroscopy,¹³ or T2*-corrected, multiecho 3D-gradient-echo Dixon-based methods, have recently been established.^{14,15} These MR-based approaches provide reliable quantification of skeletal muscle fat content, offer the ability to distinguish between IMCLs and EMCLs *in vivo*, and allow for the simultaneous evaluation of further imaging biomarkers of skeletal muscle, such as mass. We hypothesize that MR imaging (MRI)-determined differences in total fat content and lipid distribution within skeletal muscle tissue may serve as imaging biomarkers reflecting different states of impaired glucose metabolism.

In this context, we evaluated the distribution of IMCLs and EMCLs as well as total fat content in abdominal skeletal muscle by MRI using a dedicated segmentation algorithm in subjects with T2D, prediabetes and normoglycaemic controls from a population-based, cross-sectional cohort. Furthermore, we aimed to determine the distribution of IMCLs and EMCLs in these three population strata with different cardiometabolic risk factors.

2 | MATERIALS AND METHODS

2.1 | Study design and population

Subjects were derived from the KORA-FF4 study (2013-2014, $n = 2279$), the second follow-up study of a population-based survey within the Cooperative Health Research in the Region of Augsburg (KORA) survey in southern Germany. The study was approved by the ethics committee of the Bavarian Chamber of Physicians, Munich, Germany, and the local institutional review board of the Ludwig-Maximilians Universität München, Munich, Germany (EC no. 06068). Written informed consent was obtained from all participants. The design of the KORA studies has been described in detail previously.¹⁶ In brief, all participants underwent a comprehensive health assessment with standardized interviews and physical examinations. Furthermore, 400 eligible subjects underwent whole-body MRI according to previously described inclusion and exclusion criteria.¹⁶

2.2 | Glycaemic status

To determine the glycaemic status of the participants, one 75-g oral glucose tolerance test (OGTT) was performed for all subjects who had not yet been diagnosed with diabetes. According to the World Health Organization (WHO) OGTT definition, subjects were classified with an impaired glucose metabolism either with established T2D or prediabetes (impaired glucose tolerance and/or impaired fasting glucose: 2-hour plasma glucose following a 75-g OGTT ≥ 7.8 mmol/L and/or fasting plasma glucose [FPG] ≥ 5.6 mmol/L), and as healthy (normoglycaemic) controls (OGTT < 7.8 mmol/L and/or FPG < 5.6 mmol/L).¹⁷ Homeostatic model assessment of insulin resistance (HOMA-IR) was calculated for all subjects without antihyperglycaemic medication (with glucose in mass units: mg/dL).

2.3 | Anthropometric measurements and obesity

Body mass index (BMI) was calculated as weight (kg) divided by body height squared (m^2), with body weight and height both measured at the study centre. Waist circumference was measured at the smallest abdominal circumference or, in subjects with obesity, in the midpoint of the lowest rib and the upper margin of the iliac crest. Hip circumference was determined at the most protruding part of the hips to the nearest 1 mm. Obesity was defined according to the WHO definition with a BMI of $30 \text{ kg}/m^2$ as the cut-off value.¹⁸

2.4 | MRI protocol and data acquisition

MRI examinations were performed in supine position on a 3-Tesla Magnetom Skyra (Siemens Healthineers, Erlangen, Germany) using an 18-channel body surface coil in combination with a table-mounted

spine matrix coil. The complete imaging protocol as well as technical specificities have been described in detail elsewhere.¹⁶

For the segmentation of abdominal skeletal muscle, a T2*-corrected, multiecho 3D-gradient-echo Dixon-based sequence (multiecho Dixon) of the abdomen with the following parameters was used: time to repetition (TR): 8.90 ms; time to echo (TE): 1.23, 2.46, 3.69, 4.92, 6.15 and 7.38 ms; flip angle 4° ; readout echo bandwidth 1080 Hz/pixel; matrix 256×256 ; slice thickness 4 mm. Data were acquired during a breath-hold of 15 seconds. The postprocessing algorithm using the software MR LiverLab (version VD13; Siemens Healthineers, Cary, NC, USA) automatically calculated water- and fat-only images as DICOM-files from the original data of the six echoes. The obtained fat signal-fraction maps are based on the signal ratio of fat to the summed signal of water and fat (proton-density fat-fraction [PDFF]) and are corrected for the confounding effects of T2*-decay, quantitatively coding the mean PDFF in degrees of grey values of each voxel (1 intensity value = 0.1% fat content).¹⁴

Furthermore, coronal two-point Dixon gradient-echo sequences (TR 4.06 ms, TE 1.26 and 2.49 ms, flip angle 9° , slice thickness 1.7 mm, isotropic in-plane resolution 1.7 mm) were used for the identification of level L3 vertebra on axial slices by cross-reference.

2.5 | MR image analysis and skeletal muscle segmentation

The DICOM files were implemented into the commercially available software, OsiriX (version 8.5.1; Pixmeo SARL, Bernex, Switzerland), on a dedicated, offline workstation. Two trained independent observers blinded to any covariates of the subjects performed image analysis and abdominal skeletal muscle segmentation. Details of the applied segmentation approach have been described before.¹⁵ In brief, each abdominal muscle compartment (both the right and left psoas major muscle, quadratus lumborum muscle, autochthonous back muscles and rectus abdominis muscle) was manually segmented according to standardized, anatomical landmarks on one single, axial slice at the level of the lower endplate of the L3 vertebra. If the L3 vertebra was not imaged, the most caudal possible axial slice was selected. Subjects with significant image artifacts at all levels were excluded from the analysis. If artifacts were limited to level L3, the next possible cranial slice without artifacts was selected.

Interobserver and intraobserver reproducibility were assessed in a subset of 50 randomly selected subjects, being excellent for all included muscle compartments with only minor absolute and relative differences (intraclass correlation coefficient (ICC) $0.94\text{--}1.0$, $-0.2\% \pm 0.5\%$, $-2.6\% \pm 6.4\%$; ICC $0.96\text{--}1.0$, $0.0\% \pm 0.4\%$, $0.4\% \pm 3.8\%$, respectively).¹⁵

2.5.1 | Total, intramyocellular and extramyocellular fat content

All muscle compartments were segmented manually as described before using dedicated and standardized anatomical landmarks.¹⁵ Total muscle fat content was determined as mean PDFF (in %) within

each muscle compartment. It includes intramyocellular and intermyocellular-intrafascial lipids and adipose tissue and excludes surrounding, extramyocellular-extramyo-fascial adipose tissue.

IMCLs were quantified by postprocessing the segmented muscle compartments using a semiautomatic, in-house application (Matlab_R2017a; MathWorks, MA, USA) (Figure S1). This algorithm is based on the presumption that myocytes with a high amount of intramyocellular lipids do not feature an intensity value greater than approximately 200 (corresponding to 20% fat content) in PDFF maps and that every voxel with an intensity value greater than 200 additionally contains extramyocellular adipose tissue. Thus, an approved threshold value of 200 was set to quantify those voxels that comprise only myocytes with IMCLs excluding ECMLs.¹⁹ ECMLs were consecutively calculated as the difference of total abdominal skeletal muscle fat content (threshold value of 1000, corresponding to up to 100% fat content) and ICMLs, comprising predominantly extramyocellular-intramuscular fatty septa and adipose tissue within the muscle fascia.

2.5.2 | Visceral and subcutaneous adipose tissue; hepatic fat fraction

Visceral adipose tissue (VAT) and subcutaneous adipose tissue (SAT) as abdominal adipose tissue compartments were segmented and quantified (in cm²) by a semiautomated algorithm based on fuzzy clustering on one axial slice at the level of the umbilicus. Therefore, axial slices with a slice thickness of 5 mm were reconstructed based on 3D VIBE-Dixon sequences, which were assessed in the coronal direction.^{20,21}

Hepatic fat fraction (HFF) was determined using a T2*-corrected, multiecho Dixon sequence with regions of interest being placed in the right and left liver lobes (segments 8 and 2). HFF was then calculated as the average of the right and left lobe measurements.¹⁶

2.6 | Other covariates

Hypertension was determined as a systolic blood pressure of 140 mmHg or higher and/or diastolic blood pressure of 90 mmHg or higher or current intake of antihypertensive medication (given that the participant was aware of being hypertensive).^{22,23} Regarding physical activity, subjects were categorized as physically active (regular physical activity ≥ 1 h/wk) or physically inactive (irregular physical activity < 1 h/wk, almost no and no physical activity). Routine intake of lipid-lowering medication, non-steroidal anti-inflammatory drugs, and oral antihyperglycaemic as well as antihypertensive agents, was similarly evaluated by self-report. Smoking status was classified by self-report as never-smoker, ex-smoker and current (regular or sporadic) smoker.

2.7 | Statistical analysis

Baseline characteristics of the study population are presented as median with first and third quartile (interquartile range [IQR]) for

continuous variables and absolute counts with percentages for categorical variables. Differences in median values or counts between subjects with diabetes, prediabetes and healthy controls were assessed by Kruskal-Wallis' equality-of-populations rank test (quantitative data) or χ^2 -test (qualitative data). Correlations of IMCLs and EMCLs with cardiometabolic risk factors were evaluated by scatter plots and Spearman's rho correlation coefficients, and differences according to glycaemic status were evaluated by Kruskal-Wallis test. Associations of IMCLs and EMCLs with cardiometabolic risk factors were determined by median regression adjusted for age and gender. Statistical significance was indicated by *P* values of less than .05. Statistical analysis was performed using R version 3.4.1 (R Core Team; www.r-project.org, 2017).

3 | RESULTS

3.1 | Study population

Among 400 subjects who underwent whole-body MRI, 63 subjects (15.8%) were excluded because of insufficient image quality, incomplete MRI datasets of one of the sequences included, or because of missing values in any of the covariates. Thus, the study cohort consisted of 337 subjects (median 56.0 [IQR: 49.0-64.0] years, 56.4% males, median BMI: 27.2 kg/m²). Demographics and detailed characteristics of the study population are provided in Table S1.

Overall, 129 subjects (38.3%) were classified with an impaired glucose metabolism (established T2D: 49 subjects [14.5%] and prediabetes: 80 subjects [23.7%], respectively). These subjects with prediabetes and T2D featured a more distinct cardiometabolic risk profile, being older and more probably male, having a higher prevalence of obesity, hypertension and dyslipidaemic changes of blood lipids, as well as higher amounts of VAT and SAT. Furthermore, participants with impaired glucose metabolism were significantly less physically active (all *P* < .002; Table S1).

3.2 | Total, intramyocellular and extramyocellular fat content

Detailed results of measurements of total, intramyocellular and extramyocellular fat content are provided in Table 1. Median total fat content in all muscle compartments was 9.6% (IQR: 7.7%-12.7%) in normal-weight subjects and 13.4% (IQR: 10.4%-16.1%) in subjects with obesity (*P* < .001). In subjects with and without obesity, total fat content, IMCLs and EMCLs were lowest in the quadratus lumborum muscle (normal weight: total fat content 5.4% [IQR: 3.7%-7.5%], IMCLs 3.8% [IQR: 2.9%-4.9%] and EMCLs 1.4% [IQR: 0.4%-2.7%]; obesity: total fat content 6.6% [IQR: 5.1%-9.2%], IMCLs 4.2% [IQR: 3.3%-5.2%] and EMCLs 2.4% [IQR: 1.0%-3.9%]; *P* < .001, respectively) and highest in the autochthonous back muscles (normal weight: total fat content 14.0% [IQR: 9.7%-18.0%], IMCLs 7.0% [IQR: 5.7%-8.7%] and EMCLs 6.4% [IQR: 3.9%-9.3%]; obesity: total fat content 17.7%

TABLE 1 Total, intramyocellular and extramyocellular fat content in abdominal skeletal muscle

	All subjects			Normoglycaemic controls		Prediabetes		T2D		P value
	Normal weight ^a N = 241	Obese ^a N = 96		Normal weight ^a N = 171	Obese ^a N = 37	Normal weight ^a N = 45	Obese ^a N = 35	Normal weight ^a N = 25	Obese ^a N = 24	
Psoas major	Total fat content	6.5 [4.9, 8.3]	8.1 [6.4, 10.2]	5.9 [4.8, 8.0]	7.1 [6.5, 9.9]	7.5 [5.9, 9.5]	6.8 [5.8, 9.5]	8.5 [6.4, 10.4]	9.5 [8.2, 10.9]	<.001
	IMCL	4.7 [3.9, 6.5]	5.5 [4.7, 6.9]	4.5 [3.8, 5.8]	5.4 [4.3, 6.5]	6.0 [4.2, 7.0]	5.1 [4.3, 6.3]	6.7 [4.8, 7.4]	6.8 [5.8, 7.6]	<.001
	EMCL	1.4 [0.8, 2.5]	2.2 [1.3, 3.3]	1.3 [0.7, 2.3]	1.9 [1.3, 3.4]	1.4 [0.9, 2.5]	2.1 [1.2, 2.9]	1.8 [1.0, 3.2]	2.6 [1.3, 3.4]	.001
Quadratus lumborum	Total fat content	5.4 [3.7, 7.5]	6.6 [5.1, 9.2]	4.8 [3.4, 7.0]	6.3 [5.5, 7.4]	6.2 [5.0, 9.0]	7.1 [4.6, 9.7]	6.4 [5.4, 8.9]	7.3 [4.9, 12.7]	<.001
	IMCL	3.8 [2.9, 4.9]	4.2 [3.3, 5.2]	3.6 [2.9, 4.7]	4.2 [3.6, 5.0]	4.3 [3.4, 5.6]	3.8 [3.1, 4.9]	4.4 [3.2, 6.2]	5.0 [3.7, 6.7]	.002
	EMCL	1.4 [0.4, 2.7]	2.4 [1.0, 3.9]	1.2 [0.3, 2.3]	2.3 [1.2, 2.9]	1.8 [0.7, 3.0]	2.3 [1.0, 4.5]	2.5 [0.8, 4.9]	2.8 [1.0, 4.9]	<.001
Autochthonous back muscles	Total fat content	14.0 [9.7, 18.0]	17.7 [13.0, 22.5]	13.0 [9.4, 17.3]	15.9 [11.7, 20.0]	14.2 [11.1, 17.4]	18.2 [13.0, 22.9]	16.6 [12.9, 25.4]	20.3 [15.8, 26.5]	<.001
	IMCL	7.0 [5.7, 8.7]	8.6 [6.5, 10.2]	6.8 [5.4, 8.2]	8.2 [6.5, 9.6]	7.6 [6.2, 8.7]	8.4 [6.2, 10.2]	8.8 [7.1, 9.8]	9.1 [7.9, 10.7]	<.001
	EMCL	6.4 [3.9, 9.3]	9.4 [5.5, 12.4]	6.0 [3.7, 9.1]	6.8 [4.8, 10.5]	6.3 [4.6, 8.7]	10.4 [6.1, 12.4]	8.5 [5.3, 16.2]	10.6 [7.1, 14.7]	<.001
Rectus abdominis	Total fat content	12.0 [7.9, 18.5]	16.9 [12.1, 24.1]	11.3 [7.7, 16.9]	16.2 [10.9, 23.0]	14.0 [9.2, 18.2]	16.9 [12.6, 22.8]	14.7 [9.8, 20.6]	18.2 [14.1, 27.7]	<.001
	IMCL	6.8 [4.9, 8.9]	8.3 [6.1, 10.5]	6.7 [4.9, 8.4]	8.3 [5.9, 10.5]	6.8 [5.6, 9.6]	7.5 [6.5, 9.9]	7.6 [5.0, 9.9]	8.7 [6.3, 10.9]	.02
	EMCL	5.1 [2.5, 9.9]	7.4 [5.0, 15.0]	4.6 [2.1, 8.7]	7.2 [4.3, 13.3]	6.0 [2.7, 10.7]	8.3 [5.2, 14.9]	7.8 [3.1, 11.1]	9.4 [5.8, 18.4]	<.001
All muscle compartments	Total fat content	9.6 [7.7, 12.7]	13.4 [10.4, 16.1]	9.0 [7.2, 11.7]	12.5 [8.6, 15.5]	10.6 [8.7, 13.7]	13.0 [11.3, 15.2]	11.6 [10.3, 14.2]	15.8 [11.9, 17.0]	<.001
	IMCL	5.7 [4.8, 7.0]	6.7 [5.8, 8.2]	5.5 [4.6, 6.5]	6.4 [5.5, 8.0]	6.3 [5.1, 8.0]	6.5 [5.4, 7.4]	7.0 [5.5, 8.4]	7.7 [6.4, 8.9]	<.001
	EMCL	4.1 [2.7, 5.8]	6.7 [4.1, 8.5]	3.6 [2.4, 5.3]	5.2 [3.5, 8.3]	4.5 [3.3, 5.9]	6.8 [4.6, 7.9]	5.5 [4.4, 6.5]	7.1 [5.4, 9.2]	<.001

Note: Data are presented as median [first quartile, third quartile] with P values derived from Kruskal-Wallis test.

Abbreviations: EMCL, extramyocellular lipids; IMCL, intramyocellular lipids; T2D, type 2 diabetes.

^aObesity according to the WHO definition: body mass index ≥ 30 kg/m².

[IQR: 13.0%-22.5%], IMCLs 8.6% [IQR: 6.1%-10.5%] and EMCLs 7.4% [IQR: 5.0%-15.0%]; $P < .001$, respectively).

In general, IMCLs were significantly higher than EMCLs in normal-weight subjects (IMCLs: 5.7% vs. EMCLs: 4.1%), whereas the amounts of IMCLs and EMCLs were shown to be equal and significantly higher in subjects with obesity (6.7% for both IMCLs and EMCLs) ($P < .001$). Also, both subjects with and without obesity with impaired glucose metabolism had significantly higher amounts of IMCLs and EMCLs compared with normoglycaemic controls in all muscle compartments ($P < .001$) (Table 1). In general, subjects with obesity and with T2D had the highest amounts of total myosteatosis, IMCLs and EMCLs, whereas normoglycaemic and

normal-weight subjects had the lowest amounts of intramuscular fat (Figures 1 and S1).

3.3 | Correlations and predictors of intramyocellular and extramyocellular fat content

Results of univariable analysis of correlations between subjects' demographics and characteristics with IMCLs and EMCLs are shown in Table 2. In univariable analysis, cardiometabolic risk factors, such as age, measures of obesity (BMI, waist and hip circumference, VAT and SAT) and hypertension, were significantly and positively correlated

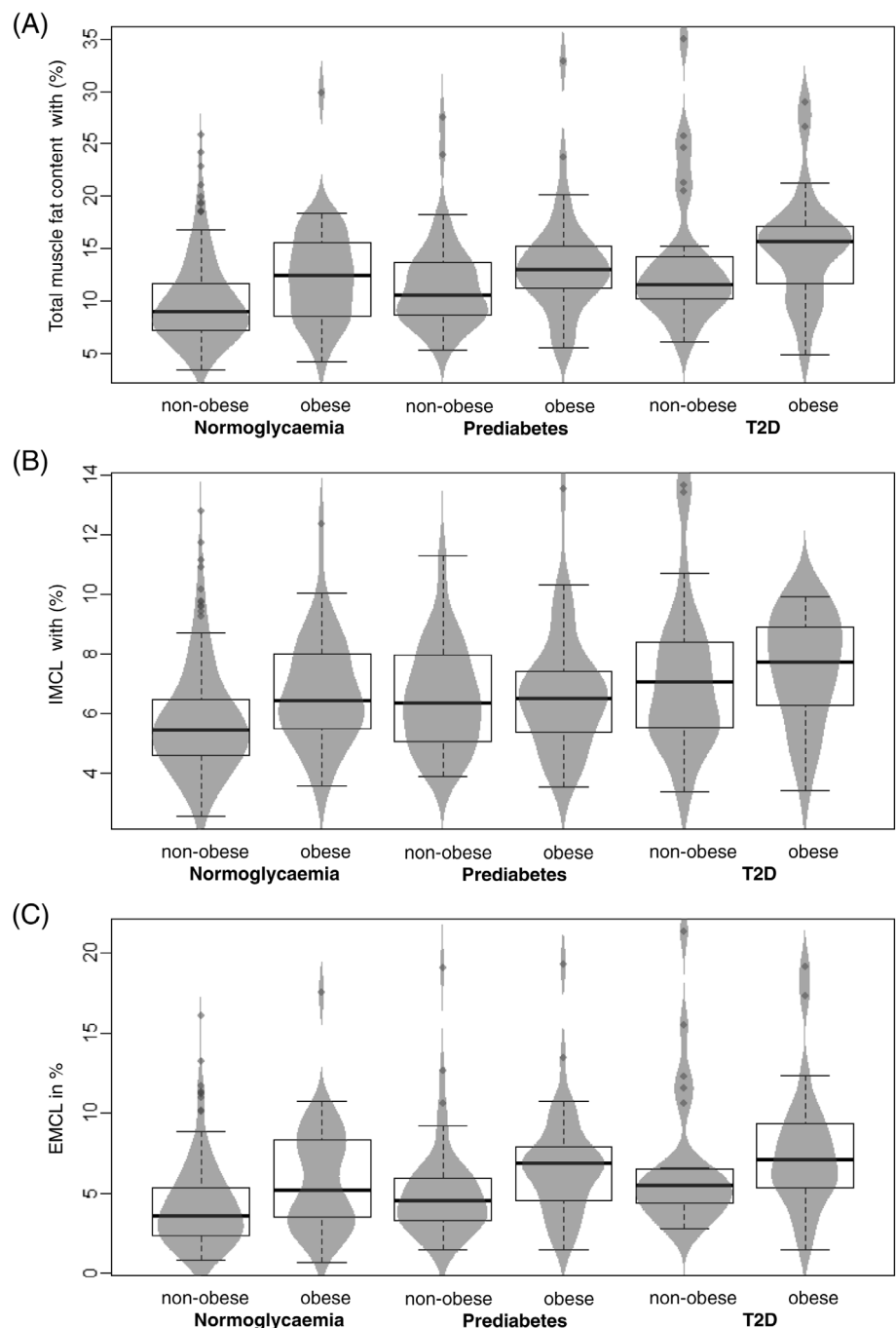


FIGURE 1 Total (A), intramyocellular (B) and extramyocellular fat content (C) in abdominal skeletal muscle in non-obese and obese subjects with type 2 diabetes (T2D), prediabetes and normal glucose tolerance. EMCL, extramyocellular lipids; IMCL, intramyocellular lipids

with the amounts of IMCLs and EMCLs (all $P < .001$) (Figure 2). A negative correlation of gender and intramuscular fat was observed for EMCLs but not for IMCLs ($P = .01$ and $P = .28$, respectively). Regarding dyslipidaemic changes of circulating blood lipids, elevated triglyceride levels and total cholesterol were significantly correlated with IMCLs (and not with EMCLs) ($P < .02$). Furthermore, regular intake of lipid-lowering medication and EMCLs, as well as of non-steroidal anti-inflammatory drugs and both IMCLs and EMCLs, were shown to be significantly correlated ($P < .03$). By contrast, there was a significant but negative correlation of both IMCLs as well as EMCLs with physical activity (Figure 2). Considering all muscle compartments, diabetes duration was not significantly correlated with total muscle fat content (Spearman's $\rho = -0.03$, $P = .88$), IMCL ($\rho = 0.02$, $P = .9$) or EMCL ($\rho = -0.04$, $P = .83$).

Regarding impaired glucose metabolism, elevated HbA1c and glucose levels, and especially the two pathological conditions, prediabetes and established T2D itself, were shown to be significantly and positively associated with the amounts of IMCLs and EMCLs in unadjusted analysis ($P < .03$). However, after adjustment for age and gender, the association of IMCL with prediabetes attenuated ($P = .06$), whereas for established T2D, both IMCLs and EMCLs remained significantly and positively associated ($P < .02$). Furthermore, obesity was significantly and positively associated with IMCLs and EMCLs in both unadjusted and adjusted analysis ($P > .002$) (Table 3A). Analysis of interaction effects between glycaemic status and obesity revealed significant associations of obesity with both IMCLs and EMCLs in subjects with normal

TABLE 2 Univariable analysis of associations between demographics and cardiometabolic risk factors with IMCLs and EMCLs

Predictor	Estimate (beta)		95% CI		P value	
	IMCL	EMCL	IMCL	EMCL	IMCL	EMCL
Age (y)	0.74	1.14	[0.54, 0.94]	[0.78, 1.50]	<0.001	<0.001
Gender (male)	-0.26	-1.23	[-0.74, 0.21]	[-2.12, -0.34]	0.28	0.01
BMI (kg/m ²)	0.63	1.08	[0.40, 0.87]	[0.78, 1.38]	<0.001	<0.001
Obesity	1.02	2.59	[0.52, 1.53]	[1.61, 3.58]	<0.001	<0.001
Waist circumference (cm)	0.60	0.95	[0.40, 0.80]	[0.70, 1.20]	<0.001	<0.001
Hip circumference (cm)	0.47	0.97	[0.27, 0.66]	[0.60, 1.34]	<0.001	<0.001
Hypertension	1.05	1.80	[0.50, 1.59]	[1.00, 2.59]	<0.001	<0.001
Systolic blood pressure (mmHg)	0.46	0.57	[0.24, 0.68]	[0.29, 0.85]	<0.001	<0.001
Diastolic blood pressure (mmHg)	0.12	0.23	[-0.10, 0.33]	[-0.12, 0.58]	0.283	0.201
Diabetes status						
Healthy control	Ref	Ref	Ref	Ref	Ref	Ref
Prediabetes	0.76	1.54	[0.28, 1.24]	[0.56, 2.51]	0.002	0.002
T2D	1.56	2.15	[0.66, 2.47]	[1.33, 2.96]	<0.001	<0.001
Physically active (regularly, ≥ 1 h/wk)	-0.71	-0.82	[-1.34, -0.08]	[-1.61, -0.03]	0.03	0.04
HbA1c (%)	0.57	0.77	[0.07, 1.08]	[0.07, 1.47]	0.03	0.03
Fasting serum glucose (mg/dL)	0.53	0.68	[0.18, 0.88]	[0.30, 1.06]	0.003	<0.001
Triglyceride levels (mg/dL)	0.39	0.27	[0.14, 0.63]	[-0.00, 0.54]	0.002	0.06
Total cholesterol (mg/dL)	0.22	0.22	[0.04, 0.40]	[-0.08, 0.51]	0.02	0.15
HDL (mg/dL)	-0.02	-0.07	[-0.24, 0.19]	[-0.46, 0.33]	0.82	0.74
LDL (mg/dL)	0.13	0.03	[-0.05, 0.30]	[-0.35, 0.41]	0.15	0.88
Medication						
Lipid-lowering medication	0.91	2.04	[-0.06, 1.88]	[0.76, 3.31]	0.07	0.002
Non-steroidal anti-inflammatory drugs	2.15	2.47	[1.63, 2.67]	[0.32, 4.62]	<0.001	0.03
Oral antihyperglycaemic agents	1.98	2.14	[1.16, 2.80]	[0.88, 3.40]	<0.001	<0.001
Oral antihypertensive agents	0.99	2.29	[0.37, 1.61]	[1.18, 3.39]	0.002	<0.001
Hepatic fat fraction (%)	0.53	0.67	[0.19, 0.87]	[0.15, 1.19]	0.003	0.01
VAT (cm ²)	0.75	0.92	[0.43, 1.06]	[0.57, 1.27]	<0.001	<0.001
SAT (cm ²)	0.56	1.22	[0.38, 0.73]	[0.84, 1.60]	<0.001	<0.001

Note: β -coefficients derived from median regression. Continuous predictors were standardized before analysis.

Abbreviations: BMI, body mass index; CI, confidence interval; EMCL, extramyocellular lipids; hypertension, $RR_{sys} \geq 140$ mmHg and/or $RR_{dia} \geq 90$ mmHg, or current intake of antihypertensive medication; IMCL, intramyocellular lipids; obesity, BMI > 30 kg/m²; SAT, subcutaneous adipose tissue; T2D, type 2 diabetes; VAT, visceral adipose tissue.

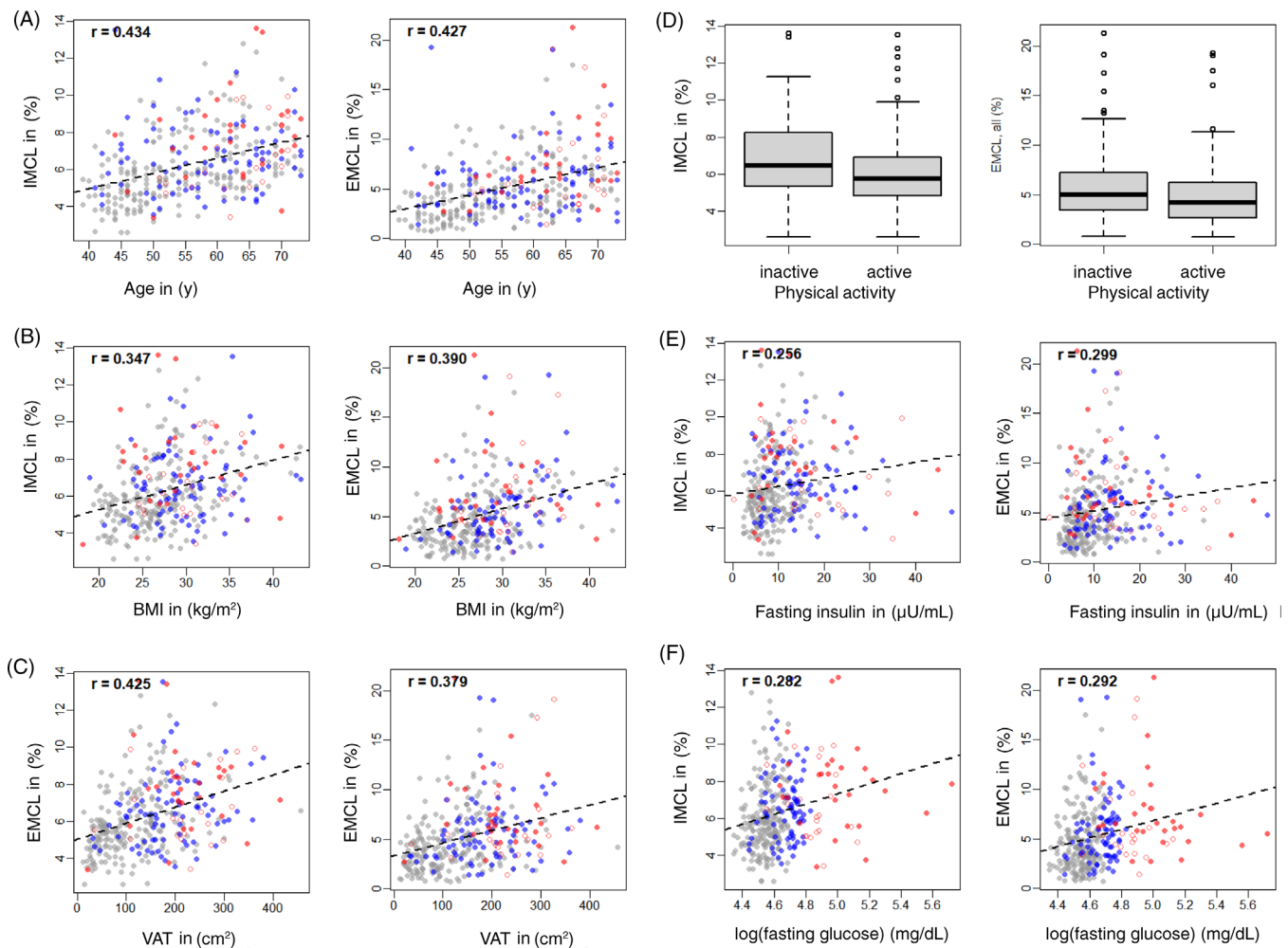


FIGURE 2 Correlations and distributions of intramyocellular and extramyocellular fat content with age (A), body mass index (BMI) (B), visceral adipose tissue (VAT) (C), physical activity (inactive: irregular physical activity <1 h/wk, almost no and no physical activity; active: regular physical activity ≥1 h/wk) (D), fasting insulin (E) and fasting glucose (F); grey = normoglycaemia; blue = prediabetes; red = diabetes (○no oral antihyperglycaemic medication, ●oral antihyperglycaemic medication). EMCL, extramyocellular lipids; IMCL, intramyocellular lipids

glucose tolerance and T2D ($P < 0.04$), but not in subjects with prediabetes (Table 3B).

4 | DISCUSSION

Disruption of muscular glucose and lipid homeostasis is assumed to be crucial in the development of prediabetes and T2D. Thereby, changes in skeletal muscle fat content as well as lipid distribution within muscle tissue are expected to be linked to peripheral insulin sensitivity. Recent data suggested a correlation of insulin resistance and myosteatosis in subjects with normoglycaemia and diabetes as well as in subjects with and without obesity. However, data on muscular fat content and lipid distribution patterns within abdominal skeletal muscle in a population-based cohort are missing to date. Our results indicate that there are significant differences in total muscle fat content and muscular lipid distribution between subjects of normal weight and subjects with obesity with T2D, prediabetes and

normoglycaemia, which may be assessed non-invasively by MRI. Patterns of intramuscular fat distribution and insulin sensitivity-related differences as assessed by MRI show potential as feasible imaging biomarkers in impaired glucose metabolism and also other metabolic diseases.

IMCLs and EMCLs represent ectopic lipid storages in two different compartments within muscle tissue. On the one hand, IMCLs constitute an important, fast available source of energy during muscle contraction and regeneration.²⁴ On the other hand, EMCLs represent a rather long-term storage, which is built up in cases of excess fat availability.^{8,9} IMCLs have recently been implicated in the pathogenesis of skeletal muscle insulin resistance.¹⁰ However, elevated amounts of IMCLs also occur in trained athletes²⁵ and in other cases of enhanced fat oxidation. Thereby, IMCLs do not adversely affect muscular insulin sensitivity but exhibit an essential function for skeletal muscle metabolism and physical capability.²⁶ In agreement with that, normal-weight subjects (who were also significantly more physically active) showed higher amounts of IMCLs compared with EMCLs in all

TABLE 3 (A) Multivariable associations between the glycaemic status and IMCLs/EMCLs and (B) interactive effects of glycaemic status and obesity

	Estimate (beta)		95% CI		P value	
	IMCL	EMCL	IMCL	EMCL	IMCL	EMCL
(A)						
Univariable/not adjusted						
<i>Model 1</i>						
Normoglycaemia	Ref	Ref	Ref	Ref	Ref	Ref
Prediabetes	0.76	1.54	[0.28, 1.24]	[0.56, 2.51]	.002	.002
T2D	1.56	2.15	[0.66, 2.47]	[1.33, 2.96]	<.001	<.001
<i>Model 2</i>						
Normal weight	Ref	Ref	Ref	Ref	Ref	Ref
Obesity	1.02	2.59	[0.52, 1.53]	[1.61, 3.58]	<.001	<.001
Adjusted for age and gender						
<i>Model 1</i>						
Normoglycaemia	Ref	Ref	Ref	Ref	Ref	Ref
Prediabetes	0.49	1.02	[-0.01, 0.99]	[0.42, 1.63]	.06	.001
T2D	1.31	1.71	[0.25, 2.38]	[0.92, 2.50]	.02	<.001
<i>Model 2</i>						
Normal weight	Ref	Ref	Ref	Ref	Ref	Ref
Obesity	0.84	1.63	[0.32, 1.35]	[0.88, 2.37]	.002	<.001
(B)						
<i>Normoglycaemia</i>						
Normal weight	Ref	Ref	Ref	Ref	Ref	Ref
Obesity	0.92	1.47	[0.33, 1.52]	[0.10, 2.84]	.002	.04
<i>Prediabetes</i>						
Normal weight	0.84	0.88	[0.22, 1.46]	[-0.05, 1.80]	.008	.06
Obesity	0.37	1.47	[-0.32, 1.06]	[-0.11, 3.06]	.29	.07
<i>T2D</i>						
Normal weight	0.79	1.15	[-0.54, 2.11]	[-0.00, 2.31]	.25	.05
Obese	1.82	2.59	[0.62, 3.03]	[1.43, 3.75]	.003	<.001

Note: β -coefficients with 95% CIs derived from median regression (A) and β -coefficients with 95% CIs derived from median regression, adjusted for age and gender (B).

Abbreviations: CI, confidence interval; EMCL, extramyocellular lipids; IMCL, intramyocellular lipids; obesity: body mass index > 30 kg/m²; T2D, type 2 diabetes.

muscle compartments, whereas subjects with obesity had both higher amounts of IMCLs and EMCLs in our study. These different patterns of muscular lipid distribution may be feasible imaging markers in physiological as well as in impaired skeletal muscle metabolism.

Previously published results by Jacob et al. showed that IMCLs were significantly higher in insulin-resistant individuals compared with insulin-sensitive subjects. Thus, they concluded that elevated IMCLs may represent an early abnormality in the pathogenesis of muscular insulin resistance.¹² In our cohort, we also found a significant association of IMCLs, in both prediabetes and T2D, in unadjusted analysis. However, after adjusting for age and gender, the association of IMCLs and prediabetes was attenuated. One explanation for this discrepancy, in comparison with the results from Jacob et al., may be the

complexity of skeletal muscle metabolic dysfunction in metabolic syndrome, specifically in the setting of co-morbidities of diabetes, obesity and other cardiometabolic diseases. In our cohort, subjects with impaired glucose tolerance also showed a significantly more distinct cardiometabolic risk profile. Furthermore, and in contrast to the study conducted by Jacob et al., different glycaemic status groups were not matched for cardiometabolic risk factors. Because skeletal muscle lipid and glucose metabolism are dynamically linked, an increased BMI as a general measure for obesity may thereby confound the association of IMCLs and muscular insulin resistance. These results may further support the theory of mutual reactions of dyslipidaemia and dysglycaemia, resulting in both hyperglycaemic and hyperlipidaemic muscle fat infiltration. Still,

whether IMCLs are causally linked to insulin resistance is a matter of considerable debate and should be addressed in further, large-scale studies.

Because obesity leads to significant fat maldistribution within the human body, ectopic lipid deposits, for example in the liver or in skeletal muscle, have recently moved into focus. Subjects with obesity in our study were not only characterized by significantly higher amounts of total muscle fat content and IMCLs, but also EMCLs in all muscle compartments and in all three glycaemic status groups compared with the normal-weight groups. Also, different measures of obesity and especially elevated amounts of VAT and SAT or hepatic fat fraction (as other cardiometabolic imaging biomarkers) were significantly associated with both IMCLs and EMCLs. Furthermore, increased peripheral lipid availability (e.g. elevated plasma triglyceride or cholesterol levels) was shown to be significantly associated with IMCLs. These correlations further highlight the complex relationship of glucose and lipids in different metabolic co-morbidities (especially T2D and obesity). Evaluating skeletal muscle biomarkers by MRI, as assessed in the current study, may therefore help to further characterize muscular changes in metabolic disorders and also elucidate the relationship between insulin resistance and intramyocellular fat components.

Some limitations of this study should be taken into account. First, we did not compare the results of muscular fat quantification by MRI with histopathology, which is seen as the current gold standard. However, former studies have shown the validity and reproducibility of the multiecho Dixon-based method used in this study.¹⁵ Second, as mentioned above, the three glycaemic status groups were not fully matched with respect to age, gender and measures of obesity. However, while multivariable analysis was used to adjust for potential confounders, our findings are limited by a comparatively small sample size (second follow-up study) from a southern German population and the cross-sectional study design, and thus require confirmation in larger and longitudinal cohort studies, for example, the German National Cohort MRI study.^{27,28}

In conclusion, we found significant differences in total muscle fat content, IMCLs and EMCLs between subjects with normal weight and obesity with T2D, prediabetes and normoglycaemic controls that may be assessed non-invasively by MRI. Different patterns of intramuscular fat distribution may therefore be regarded as feasible imaging biomarkers in impaired glucose metabolism and other metabolic diseases and may further elucidate a 'muscular phenotype' associated with an increased cardiometabolic risk. This might enable 'muscular phenomapping' by MRI in, for example, early detection of glucose and lipid metabolism disruption.

CONFLICT OF INTEREST

None.

PEER REVIEW

The peer review history for this article is available at <https://publons.com/publon/10.1111/dom.14413>.

DATA AVAILABILITY STATEMENT

Data available on request from the authors

ORCID

Lena S. Kiefer  <https://orcid.org/0000-0002-3999-559X>

REFERENCES

- Häring HU, Mehnert H. Pathogenesis of type 2 (non-insulin-dependent) diabetes mellitus: candidates for a signal transmitter defect causing insulin resistance of the skeletal muscle. *Diabetologia*. 1993; 36:176-182.
- Randle PJ, Garland PB, Hales CN, Newsholme EA. The glucose fatty-acid cycle - its role in insulin sensitivity and the metabolic disturbances of diabetes mellitus. *Lancet*. 1963;281:785-789.
- McGarry JD. Dysregulation of fatty acid metabolism in the etiology of type 2 diabetes. *Diabetes*. 2002;51:7-18.
- Brehm A, Krssak M, Schmid AI, Nowotny P, Waldhausl W, Roden M. Increased lipid availability impairs insulin-stimulated ATP synthesis in human skeletal muscle. *Diabetes*. 2006;55:136-140.
- Kelley DE, Mandarín LJ. Fuel selection in human skeletal muscle in insulin resistance: a reexamination. *Diabetes*. 2000;49:677-683.
- DeFronzo RA, Tripathy D. Skeletal muscle insulin resistance is the primary defect in type 2 diabetes. *Diabetes Care*. 2009;32:157-163.
- Perseghin G, Scifo P, de Cobelli F, et al. Intramyocellular triglyceride content is a determinant of in vivo insulin resistance in humans. *Diabetes*. 1999;48:1600-1606.
- Chalkley SM, Hettiarachchi M, Chisholm DJ, Kraegen EW. Five-hour fatty acid elevation increases muscle lipids and impairs glycogen synthesis in the rat. *Metabolism*. 1998;47:1121-1126.
- Brechtel K, Dahl DB, Machann J, et al. Fast elevation of the intramyocellular lipid content in the presence of circulating free fatty acids and hyperinsulinemia: a dynamic ¹H-MRS study. *Magn Reson Med*. 2001;45:179-183.
- Virkamäki A, Korshennikova E, Seppälä-Lindroos A, et al. Intramyocellular lipid is associated with resistance to in vivo insulin actions on glucose uptake, antilipolysis, and early insulin signaling pathways in human skeletal muscle. *Diabetes*. 2001;50:2337-2343.
- Boden G, Chen X. Effects of fat on glucose uptake and utilization in patients with non-insulin-dependent diabetes. *J Clin Invest*. 1995;96:1261-1268.
- Jacob S, Machann J, Rett K, et al. Association of increased intramyocellular lipid content with insulin resistance in lean nondiabetic offspring of type 2 diabetic subjects. *Diabetes*. 1999;48:1113-1119.
- Schick F, Eismann B, Jung WJ, Bongers H, Bunse M, Lutz O. Comparison of localized proton NMR signals of skeletal muscle and fat tissue in vivo: two lipid compartments in muscle tissue. *Magn Reson Med*. 1993;29:158-167.
- Fischer MA, Nanz D, Shimakawa A, et al. Quantification of muscle fat in patients with low back pain: comparison of multi-echo MR imaging with single-voxel MR spectroscopy. *Radiology*. 2013;266:555-563.
- Kiefer LS, Fabian J, Lorbeer R, et al. Inter- and intraobserver variability of an anatomical landmark-based, manual segmentation method by MRI for the assessment of skeletal muscle fat content and area in subjects from the general population. *Br J Radiol*. 2018;91:1-9.
- Bamberg F, Hetterich H, Rospleszcz S, et al. Subclinical disease burden as assessed by whole-body MRI in subjects with prediabetes, subjects with diabetes, and normal control subjects from the general population: the KORA-MRI study. *Diabetes*. 2017;66:158-169.
- World Health Organization. *Definition and Diagnosis of Diabetes Mellitus and Intermediate Hyperglycemia*; Geneva, Switzerland: World Health Organization; 2006:1-50.

18. World Health Organization. *Obesity: Preventing and Managing the Global Epidemic* (WHO Technical Report Series 894). Geneva, Switzerland: World Health Organization; 2000.
19. Boettcher M, Machann J, Stefan N, et al. Intermuscular adipose tissue (IMAT): association with other adipose tissue compartments and insulin sensitivity. *J Magn Reson Imaging*. 2009;29:1340-1345.
20. Würsli C, Machann J, Rempp H, Claussen C, Yang B, Schick F. Topography mapping of whole body adipose tissue using a fully automated and standardized procedure. *J Magn Reson Imaging*. 2010;31:430-439.
21. Schwenzer NF, Machann J, Schraml C, et al. Quantitative analysis of adipose tissue in single transverse slices for estimation of volumes of relevant fat tissue compartments: a study in a large cohort of subjects at risk for type 2 diabetes by MRI with comparison to anthropometric data. *Invest Radiol*. 2010;45:788-794.
22. World Health Organization. *A Global Brief on Hypertension*. Geneva, Switzerland: World Health Organization; 2013:1-40.
23. Heidelberg DL zur B, des Hohen BEV. Empfehlungen zur Hochdruckbehandlung in der Praxis und zur Therapie hypertensiver Notfälle, 20; 2010.
24. Brechtel K, Niess AM, Machann J, et al. Utilisation of intramyocellular lipids (IMCLs) during exercise as assessed by proton magnetic resonance spectroscopy (1H-MRS). *Horm Metab Res*. 2001;33:63-66.
25. Thamer C, Machann J, Bachmann O, et al. Intramyocellular lipids: anthropometric determinants and relationships with maximal aerobic capacity and insulin sensitivity. *J Clin Endocrinol Metab*. 2003;88:1785-1791.
26. Laurens C, Moro C. Intramyocellular fat storage in metabolic diseases. *Horm Mol Biol Clin Investig*. 2016;26:43-52.
27. Bamberg F, Kauczor HU, Weckbach S, et al. Whole-body MR imaging in the German National Cohort: rationale, design, and technical background. *Radiology*. 2015;277:206-220.
28. Schlett CL, Hendel T, Weckbach S, et al. Population-based imaging and radiomics: rationale and perspective of the German National Cohort MRI Study. *Rofo*. 2016;188:652-661.

SUPPORTING INFORMATION

Additional supporting information may be found online in the Supporting Information section at the end of this article.

How to cite this article: Kiefer LS, Fabian J, Rospleszcz S, et al. Distribution patterns of intramyocellular and extramyocellular fat by magnetic resonance imaging in subjects with diabetes, prediabetes and normoglycaemic controls. *Diabetes Obes Metab*. 2021;23:1868-1878. <https://doi.org/10.1111/dom.14413>